Water Resources Research

RESEARCH ARTICLE
10.1029/2024WR037523

Predicting Morphological Changes Along a Macrotidal Coastline Using a Two-Stage Machine Learning Model

Pavitra Kumar[1] and **Nicoletta Leonardi**[1]

[1]Department of Geography and Planning, School of Environmental Sciences, University of Liverpool, Liverpool, UK

Key Points:

- This study analyses real time beach transect data collected twice a year from 2007 to 2022 along Morecambe Bay coastline
- Random forest classifier is trained to classify beach behavior as: eroding, accreting, stable, or undergoing short-term fluctuations
- LSTM and sequence-to-sequence models are trained to predict the change in volume of sediment after erosion/accretion at particular beach

Supporting Information:

Supporting Information may be found in the online version of this article.

Correspondence to:

P. Kumar,
pavitra.kumar@liverpool.ac.uk

Citation:

Kumar, P., & Leonardi, N. (2025). Predicting morphological changes along a macrotidal coastline using a two-stage machine learning model. *Water Resources Research*, *61*, e2024WR037523. https://doi.org/10.1029/2024WR037523

Received 2 APR 2024
Accepted 28 MAR 2025

Author Contributions:

Conceptualization: Pavitra Kumar, Nicoletta Leonardi
Data curation: Nicoletta Leonardi
Funding acquisition: Nicoletta Leonardi
Investigation: Pavitra Kumar
Methodology: Pavitra Kumar
Project administration: Nicoletta Leonardi
Supervision: Nicoletta Leonardi
Validation: Pavitra Kumar, Nicoletta Leonardi
Writing – original draft: Pavitra Kumar
Writing – review & editing: Nicoletta Leonardi

Abstract Understanding and predicting coastal change is of the foremost importance to protect coastal communities and coastal assets. This study analyzes field data from 125 locations along the Morecambe coastline, consisting of beach transects collected twice a year for more than a decade (2007–2022). Wave data at these 125 locations were simulated using the hydrodynamic Delft3D model, with full coupling of the Delft3D FLOW and WAVE modules. To model the sediment volume changes observed along the Morecambe coastline, this study proposes a two-stage machine learning model that incorporates beach behavior classification and deep learning techniques to predict changes in sediment volumes along coastal environments. The first stage of the model, developed using a random forest classifier, classifies beach behavior into four categories: eroding, accreting, stable, or undergoing short-term fluctuations. The second stage of the model developed using LSTM and sequence-to-sequence models, uses the output of the first stage to predict the change in sediment volume after erosion/accretion. The random forest classifier achieves testing accuracy of 0.74. LSTM model achieved a testing regression of 0.92 for one-step-ahead (6 months) predictions of change in sediment volume time series, while sequence-to-sequence model achieved the testing regression of 0.96 for three-time-ahead (1.5 years) predictions and 0.88 for ten-time-step-ahead (5 years) prediction.

Plain Language Summary This study investigates how coastlines change over time. We focused on the Morecambe Bay in England and analyzed data collected over 16 years from 2007 to 2022. Artificial intelligence models were developed that learn from coastline data to predict if a beach will erode, grow bigger, stay the same or changing in small bursts. These models work in two steps: first, they classify coastlines based on their overall coastline trend (e.g., erosion vs. accretion). Then, they use that information to predict how much change in sediment volume a particular beach location will experience in 6 months, 1.5 years, or even 5 years from now. These models are capable of accurately predicting beach behavior and sediments volume changes, especially for long-term predictions.

1. Introduction

Dynamic coastal processes continuously shape the coastline and understanding coastal dynamics is important to protect coastal communities and coastal infrastructures. Waves, tidal energy, and sediment availability are key factors that determine sediment transport and drive morphological changes (Dionísio António et al., 2023; Pang et al., 2021). Anthropogenic activities that alter the delivery of sediments to coastal areas can also accelerate the rate of coastline change (Prasad & Kumar, 2014; van Rijn, 2011; Williams et al., 2018). With sea level rise and changes in storms activity, there is increased uncertainty about the risk of erosion (Boettle et al., 2013), flooding (Lyddon et al., 2019; Muñoz et al., 2020; Yin et al., 2016) and on whether the project lifetime of coastal management structures will prove adequate to withstand the challenges posed by climate change. Several soft nourishment and hard structures are designed to address coastal erosion problems. Soft nourishment includes, for instance, shoreface nourishment (beach fills) (Kumar & Leonardi, 2023c, 2024a; Pinto et al., 2022) and submerged reefs (Harris, 2012), while hard structures include groins (Lima et al., 2020), detached breakwaters (Browder et al., 2015), seawalls (Betzold & Mohamed, 2017), and revetments (Crawford et al., 2020). To be effective, these engineering solutions must be installed at identified vulnerable locations. Historic erosion and deposition data as well as predictive models can be used to identify such locations, specifically those that can be classified as having long-term chronic erosion or short-term fluctuating erosion trends. For instance, if an area of interest experiences substantial sediment loss over 5–10 years, it can be considered to have long-term chronic erosion and thus requires erosion protection measures (van Rijn, 2011).

Machine Learning models such as artificial neural networks (ANNs) and other predictive models can be useful for monitoring and nonlinear forecasting of coastal change (Kumar & Leonardi, 2023a, 2023b). Historical data, whether obtained from remote sensing or direct field campaigns, can be utilized to train these machine learning models and identify coastal changes, thereby supporting coastal management efforts. For instance, Yang et al. (2023) and Xiong et al. (2024) effectively employed machine learning models to monitor the dynamics of deltaic islands using remote sensing data from 1991 to 2019 and to track changes in mangrove forests using remote sensing data from 1988 to 2022, respectively. Similarly, Yang et al. (2023) used image-based machine leaning models to quantify the dynamic changes of deltaic islands in Wax Lake Delta (WLD) and Atchafalaya Delta (AD) in Louisiana, USA, using remote sensing images from 1991 to 2019. These machine learning models are particularly useful when long-term morphodynamical models are unavailable or computationally expensive.

ANN models are information processing systems modeled on the structure of the human brain (Anctil et al., 2009; Sharma et al., 2003) and effective in dealing with nonlinearities (Farzad & El-Shafie, 2017) and have been successfully applied to other coastal engineering problems. ANN models can learn the nonlinear relationships between the different variables that influence coastal erosion, making them well-suited for modeling this complex process. ANN models can even learn dependencies that process-based models fail to capture. Several researchers have developed models to predict coastal erosion, including Peponi et al. (2019), Corbella and Stretch (2012) and Adamo et al. (2014). Peponi et al. (2019) integrated geographic information systems (GIS) with ANN to predict erosion-prone areas at the coastal zones of Costa da Caparica in Lisbon, Portugal, in the near future. They mainly considered anthropogenic inputs from GIS, such as the number of residents, land cover, number of households, and vegetated and non-vegetated areas, to predict erosion-prone areas using ANN. Corbella and Stretch (2012) and Adamo et al. (2014) used process-based models to estimate coastal erosion. Corbella and Stretch (2012) used the SBEACH, XBEACH, and Time Convolution models to estimate coastal erosion trends at coastal areas of Durban, South Africa. Adamo et al. (2014) used directional wave spectrum and direction of wave propagation to estimate coastal erosion and used this it to estimate shoreline change.

This study proposes a combination of two machine learning models aimed at (a) classifying beach profiles based on their morphological trends and (b) predicting time series of morphological changes. Continuous field campaigns were conducted from 2007 to 2022 to collect beach profiles using GS16 Leica antenna and a Leica CS20 handset at 125 locations along Morecambe Bay. Hydrodynamic simulations for Morecambe Bay were conducted using Delft3D to obtain coastal parameters such as wave height, wave direction and wave velocity. Information from the hydrodynamic model were then fed along with historical transect data into the machine learning models. Specifically: (a) Based on field data, we construct a robust random forest classifier model that can accurately predict the long-term behavior of the coastline, categorizing it into erosional, accretional, stable, or undergoing short-term morphological fluctuations. (b) Based on field and modeling data, we developed Long Short-Term Memory (LSTM) and sequence-to-sequence model to forecast the change in volume of sediment at specific locations over time, further enhancing our ability to comprehend and anticipate coastal morphological changes.

The manuscript is organized as follows: After presenting the study site, the methodology section details the field data collection methods, hydrodynamic modeling techniques, machine learning models employed, and performance criteria used to evaluate the models' effectiveness. The results section then presents the analysis of the gathered field data and model performance. Following this, the discussion section delves into the literature on coastline change in Morecambe Bay and explores the applicability of the developed models in this context. Finally, the conclusion section summarizes the study, highlighting key findings and implications.

2. Study Site

Morecambe Bay, a macrotidal embayment in northwest England, is the test case of this study. Its shoreline is mostly covered in fine sand, and the bay opens southwest into the Irish Sea (Mason et al., 2010). Intertidal zones, especially sandbanks and subtidal channels, are highly susceptible to change, and these changes can be observed even within a single season. The fetch length is constrained by landmasses such as Ireland and the Isle of Man. As a result, significant wave heights at the bay mouth reach up to 2 m for only about 10% of the year, remaining around 0.5 m for the rest of the year. Morecambe Bay has a large ordinary spring tidal range of approximately 8.2 m and its subtidal channels experience maximum spring tide velocities of about 1.5 m per second (Mason et al., 2010). During the 1991–2007 study period, Mason et al. (2010) found that the bay experienced significant sediment movement from below mean sea level to above mean sea level. This erosion and accretion caused the

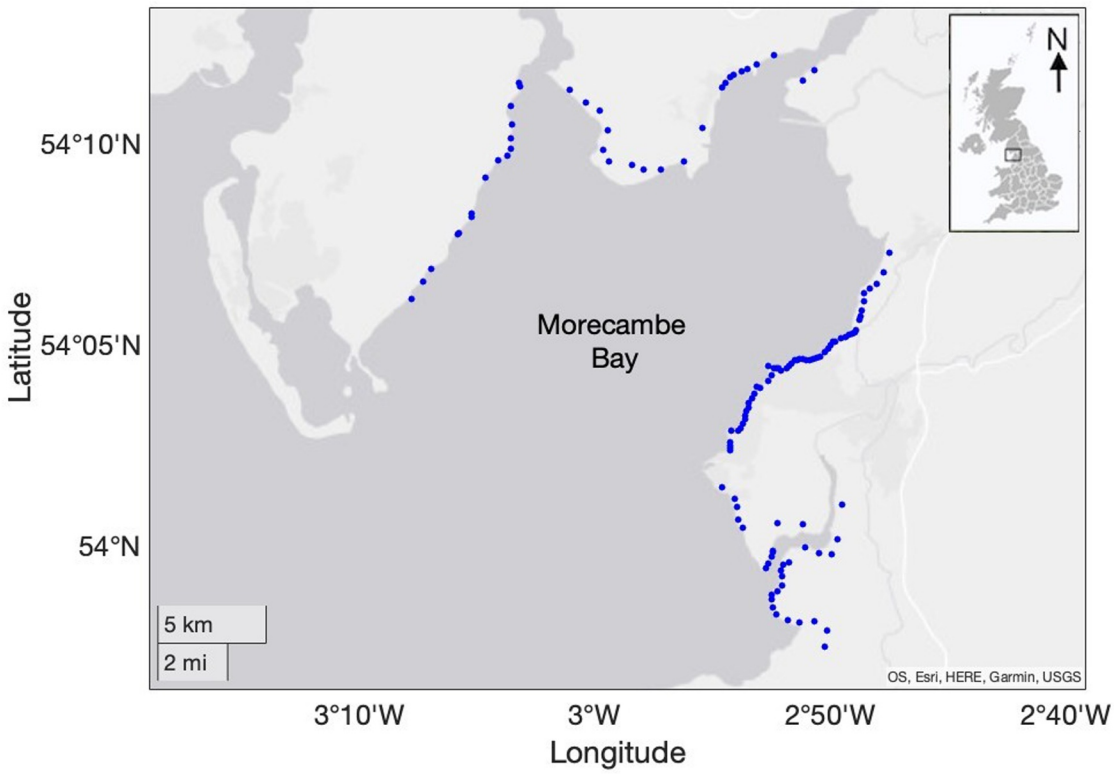

Figure 1. Location of data measurement sites (blue dots) along Morecambe coastline.

mudflat to retreat toward the landmass. Due to its dynamic behavior and significant sediment movement, this bay was selected for this study.

3. Methodology

3.1. Field Data

Sefton Council (Sefton MBC, UK) provided a data set of beach transects at 139 locations along the Morecambe Bay coastline, collected mostly between 2007 and 2022.

The raw data from Sefton Council consisted of beach transects of varying lengths, measured twice a year (spring and autumn) from 2007 to 2022 using GS16 Leica antenna and Leica CS20 handset. The data set was corrected in post processing using Lecia Infinity software with an accuracy of Hz 3 mm + 0.1 ppm/V 3.5 mm + 0.4 ppm. Locations with two or fewer transects in time and those outside Morecambe Bay were discarded, leaving 125 locations with an average of 22 transects per location (Figure 1). Some of the transect had varying length from year to year. To address this, the data were pre-processed and missed datapoints were filled with the interpolated data from the three previous transects (e.g., if part of the Autumn 2019 transect was missed, the missed section was filled through the average of the 2019 (Summer) and 2018 (spring and autumn) values (see S1 for extended explanation and table for this)). The transect data are presented in the file S1 in Supporting Information S1 and Kumar and Leonardi (2024b). This interpolation was needed for around 20% of the transects (591 out of 2883). At few locations, there were intervals in the transect data where measurements were taken with gaps in time. As presented in this file, these time gaps predominantly occurred in 2013 and 2015 at 54 locations. Moreover, for 22 locations where the initial profile was measured in 2007, there was a significant gap between 2008 and 2012. After calculating the volume of sand at each location using the area under the curve method, which provided volumes in cubic meters per meter of beach width, the sediment volumes during these missing time gaps were interpolated using spline curves. The gaps filled by this interpolation were normally one- or three-time steps. For locations with notable time gaps between 2008 and 2012, the transects from 2007 to 2008 were excluded, enabling

the transect time series to commence from 2012. A total of 256 profiles were interpolated to effectively complete the time series from 2010 to 2022 with two transects per year.

3.2. Hydrodynamic Modeling

To obtain localized wave data, we simulated the hydrodynamic in Morecambe Bay using Delft3D. From the hydrodynamic model, we extracted average and maximum wave height, average wave velocity, and wave direction at each transect location. The model was calibrated using wave buoys at Morecambe Bay, at Cleveleys and Heysham. The model boundary was forced with 10 tidal harmonics (M2, S2, N2, K2, K1, O1, P1, Q1, S1, M4) interpolated across the two boundary extremes and derived from the global tidal model GOT-e 4.10c (Ray, 1999; Stammer et al., 2014). To model realistic waves, we downloaded time-series of wave data for the Cleveleys buoy station https://www.coastalmonitoring.org/realtimedata/?chart=104&tab=download&disp_option=. We applied this wave data to the sea boundary of the simulation domain. Details about the model setup and model validation can be found in (Forrester et al., 2024; Kumar & Leonardi, 2023a, 2023c). The model grid had a variable resolution, from 120 × 130 m onshore to 1,000 × 300 m offshore. The simulation domain extended 57 km along the coastline and 20 km across, with a maximum distance from the sea boundary of 50 km. Wave and tide forcings were applied at the sea boundary, and a Neumann condition was applied at the lateral boundaries to have zero water level gradients. The wave data for the sea boundary were obtained from the Cleveleys wave station. The model was run from 2012 to 2022 at six months intervals to match the biannual data collection intervals. No time series for the wave data were available for 2010–2012 and for this period we utilized localized time-average waves parameters (average based on the 2012–2022 period). The morphology was not updated during the simulation, as the focus was on obtaining localized wave height, wave velocity, and wave direction. The simulated 2012–2022 period encompassed six storm conditions observed at Morecambe Bay: Cyclone Tini (12 February 2014) (MetOffice, 2014), Storm Barney (17–18 November 2015), Storm Clodagh (29 November 2015), Storm Desmond (03–08 December 2015), Storm Henry (1–2 February 2016) (MetOffice, 2016) and Storm Ciara (03–16 February 2020) (MetOffice, 2020). The maximum wave heights recorded during these storms were 4.84, 3.75, 4.52, 4.03, 4.6, and 4.63 m respectively. Modeling results were recorded every 30 min at observation points regularly spaced, at a distance of about 250 m, along the coastline and at a distance of about 500 m away from the starting point of beach transect measurement, which are usually on the landmass. This distance was chosen to ensure that the observation points are in the sea or in the intertidal zone, allowing for a sufficient duration of water exposure for the collection of wave data. The 125 observation points nearest to each transect were selected for data extraction. Most of the transects intersect with these observation points.

The coastline angle at each location was obtained using QGIS software, and the coastline was visually assessed using Google Earth based on vegetation presence to classify it as sandy, marshy (when vegetation is present across the whole transect), or marshy with mudflat. For some marsh areas, the length of transects were within the marshy area, so they were classified as marshy. For other locations, the length of transects was measured beyond the marshy areas into the mudflat, so they were classified as marshy with mudflat.

The wave parameters considered for further machine learning analysis include wave height, wave velocity, and wave direction. Localized maximum wave height and average wave height were both included as inputs of the ANN models.

3.3. Machine Learning Modeling

The field data and localized simulation outputs at the relevant transects were fed into the predictive models. Two predictive models were developed:

- Model A1 was developed to classify coastline behavior as erosional, accretional, stable, or undergoing short-term fluctuation based on wave direction, wave velocity, coastline angle, and coastline composition.
- Model A2 was developed to predict the change in volume of sediment after erosion/accretion based on average wave height, maximum wave height, average wave velocity, beach behavior (output of Model A1), and historical sediment volume.

Model A1 is a random forest (RF) classifier. Model A2 is based on LSTM and sequence-to-sequence models. The methodology flowchart is presented in Figure 2.

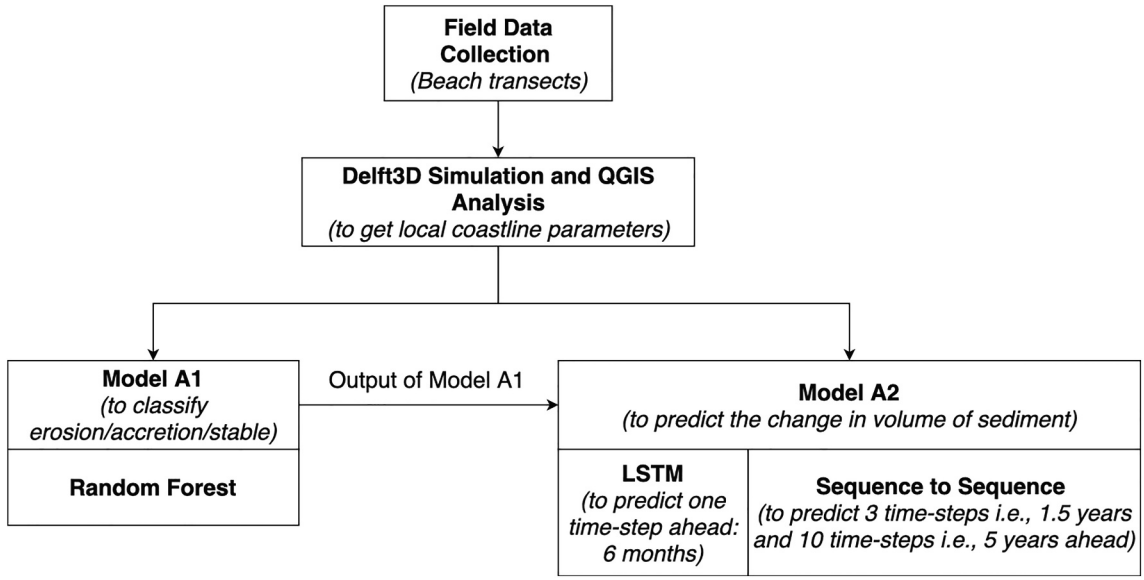

Figure 2. Flow chart of methodology.

3.3.1. Model A1

As shown in the methodology flowchart (Figure 2), field data and modeling data are fed into Model A1, which classifies beach behavior as long-term erosion, accretion, stable or short-term erosion fluctuation based on wave direction, average wave height, maximum wave height, average wave velocity, coastline angle, and coastline composition. A random forest (RF) classifier was used to classify beach behavior. RF is a machine learning algorithm that builds an ensemble of decision trees to make predictions. Decision trees are hierarchical classifiers that learn rules based on the values of input variables. RF improves the performance of decision trees by averaging the predictions of the trees, which reduces the variance of the model and makes it more robust to noise in the data. RF can be used to solve both classification and regression problems. In classification problems, the outcome is typically determined by the majority vote of the trees in the ensemble, while in regression problems, the average of the predictions of the trees in the ensemble is used. RF models are trained by resampling the training data using bootstrap sampling (Pham et al., 2022; Wei et al., 2022) or bagging (Rodriguez-Galiano et al., 2015). These methods create multiple training data sets by randomly sampling the original data with or without replacement. Training each tree on a unique subset of the training data helps to reduce the correlation between the trees (Rodriguez-Galiano et al., 2015). This is because some data points may be present in multiple subsets, while others may be excluded from all subsets. This reduced correlation makes the model more robust to variations in the input data and improves its predictive accuracy (Breiman, 2001).

The problem for this study was to train a RF model for multiclass classification on the MATLAB platform. Ensemble aggregation methods tried for this model were bagging, AdaBoostM2 (adaptive boosting for multiclass classification), LPBoost (linear programming boosting), RUSBoost (random undersampling boosting), and TotalBoost (totally collective boosting). Tree pruning was allowed based on the error. The number of trees tested was 50, 75, and 100.

The inputs consisted of coastline angle (radian), wave direction (radian), average wave height (m), maximum wave height (m), average wave velocity (m/s) and coastline composition (sandy, marshy, and marshy with mudflat), which was fed as categorical input. The target was classification of coastline behavior (long-term erosion, accretion, stable, and short-term erosion fluctuation), which was also fed as a categorical parameter. The total target comprised 121 transects, of which 47 were classified as stable, 26 as eroding, 22 as accreting, and the remaining 26 as short-term fluctuating. The output of Model A1 was used as input to Model A2 to provide a prediction of the change in volume of sediment.

3.3.2. Model A2

To develop Model A2, we tested two models: LSTM and sequence-to-sequence (S2S), both of which were built using LSTM cells. LSTM is a type of recurrent neural network (RNN) that is commonly used for modeling time series data. LSTMs are designed to learn long-term dependencies in time series data by selectively storing important information and discarding unimportant information through different gates. These models were developed to address the problems associated with RNNs, which have difficulty learning long-term dependencies due to gradient explosion and gradient vanishing (Kumar et al., 2023; Lindemann et al., 2021; Sun et al., 2022). Unlike feed-forward neural networks (FFNNs), RNNs allow for feedback of data back to the hidden layers, which creates a time lag effect that helps the model learn from previous time steps (Aslam et al., 2020). LSTM models can learn long-term dependencies in time series data using the gating mechanism in it. Kumar and Leonardi (2023b) provide a detailed discussion of the gating mechanism of LSTM models.

3.3.2.1. LSTM Model

LSTM model was developed to predict change in sediment volume one time step ahead where each time step in the transect data corresponds to 6 months. The network consisted of a feature input layer, a sequence input layer, a sequence unfolding and folding layer, LSTM layers, and two fully connected layers followed by a regression layer (as presented in figure S2.1 in Supporting Information S1). The feature input layer received feature inputs such as average and maximum wave height, average wave velocity, and coastline behavior (categorical). The sequence input layer received the previous three-time steps, equivalent to 1.5 years of sediment volume as its input. These feature and sequence inputs were combined at each time step using sequence unfolding and folding layer before feeding it to LSTM cells. The network was created and trained on a MATLAB platform. The number of LSTM layer tested were 3 and 4, each with 5, 10, 15, or 20 nodes. The cell weights were initialized using the He initializer. The cell state and hidden state of each layer were connected to the next layer in the sequence. This interconnection between cells allows LSTMs to capture and propagate information over time steps, which is crucial for modeling sequential data effectively.

3.3.2.2. Sequence-to-Sequence (S2S)

Sequence-to-Sequence (S2S) model S2S model was developed, in this study, to predict change in volume of sediment three-time step, that is, 1.5 years, ahead based on the previous three-time step of volume of sediment time series and feature inputs. The S2S model consists of an encoder layer, which extracts information from the input data (Tang et al., 2016), and a decoder layer, which generates the output data based on the learned states (Kim et al., 2020). The encoder and decoder layers of the S2S model were implemented using LSTM layers (LSTM cell in Figure 3), with 6 layers in the encoder and 3 layers in the decoder (Figure 3). All feature and sequence inputs, as discussed above for the LSTM model, were fed to the corresponding LSTM layers of S2S model. The cell state (C) and hidden state (H) of each layer were connected to the following layer in the network. The C, H, and output of the last LSTM layer in the encoder were connected to the LSTM layers in the decoder, as shown in Figure 3. The output of each layer in the decoder was connected to regression layer, which provided the output of the next three-time steps of sediment volume. The sequence input and target were selected using the sliding window technique, as illustrated in Figure 3. Time steps t-3, t-2, and t-1 were used as input to predict time steps t, $t + 1$, and $t + 2$. For the model predicting 10-time step ahead, this network structure was extended by adding more LSTM cells, along with their fully connected layer, in decoder to accommodate 10 time steps from t to $t + 9$. The number of nodes of each LSTM layers tested, in this study, varied from 5 to 50. The model architecture was manually assembled, and its connections were managed manually. The model was trained using a custom training loop on the MATLAB platform.

3.4. Performance Criteria

This study utilizes both classification and regression models. The RF classifier performs multi-class classification between four categories, while the LSTM and S2S models perform regression prediction of time series. The prediction performance of both models is evaluated using different criteria. Accuracy, precision, recall, and F1 score were used to assess the performance of the RF classifier model, while regression mean absolute error (MAE) and Nash-Sutcliffe efficiency (NSE) were used to assess the performance of the LSTM and S2S models.

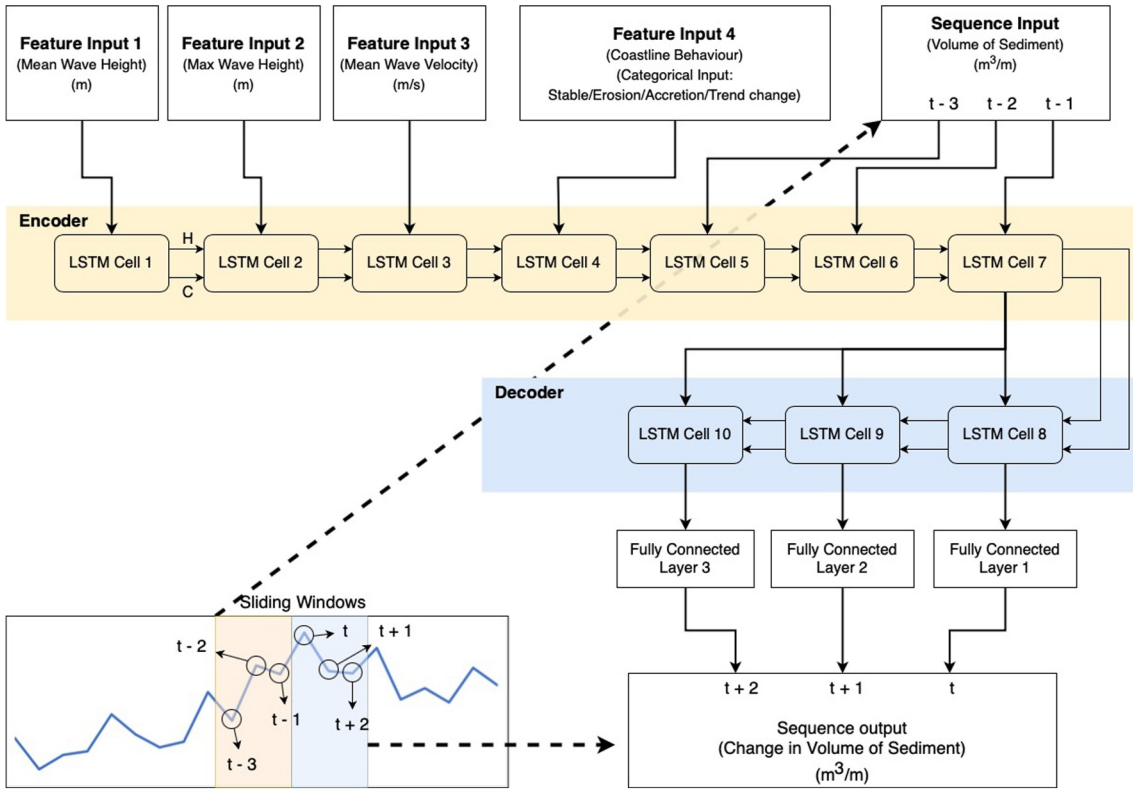

Figure 3. Model A2 structure.

Accuracy measures the model's ability to correctly classify a given observation (Equation 2). Precision measures what proportion of observations classified as positive by the model are actually positive (Equation 3), indicating how reliable the model is for positive classifications. Recall measures the model's sensitivity by calculating the percentage of items actually present in the input that were correctly identified by the model (Equation 4). F1 score measures the weighted harmonic mean of precision and recall scores (Equation 5).

$$\text{Accuracy} = \frac{\text{TP} + \text{TN}}{\text{TP} + \text{TN} + \text{FP} + \text{FN}} \tag{2}$$

$$\text{Precision} = \frac{\text{TP}}{\text{TP} + \text{FP}} \tag{3}$$

$$\text{Recall} = \frac{\text{TP}}{\text{TP} + \text{FN}} \tag{4}$$

$$F_\beta = \frac{\left(\beta^2 + 1\right) * \text{Precision} * \text{Recall}}{\beta^2 * \text{Precision} * \text{Recall}} \tag{5}$$

where: TP = true positive that is, positive observation correctly classified as positive; TN = true negative that is, negative observation correctly classified as negative; FP = false positive that is, negative observation wrongly classified as positive; FN = false negative that is, positive observation wrongly classified as negative; β is the weightage factor between precision and recall. For this study $\beta = 1$ which gives equal weightage to the precision and recall, hence F_1. Equations 2–5 are designed for binary classifications, but this study involves multi-class classification with four categories: erosion, accretion, stable, and short-term fluctuation. When the model correctly classifies an erosion beach as erosion, it is considered as a true positive. However, if the model classifies any other category as erosion, it is counted as a false positive. This process applies to all four categories. In multi-class classification, a weighted average approach is employed, where precision, recall, and F1 scores are

calculated for each category and then averaged weighting according to the number of samples in each category present in the data set.

The performance of regression models is evaluated using various metrics, including regression (Equation 6), MAE (Equation 7), and NSE (Equation 8). Regression provides a statistical measure of how closely the predicted data aligns with the target data, indicating the model's generalizing ability. MAE quantifies the error in the predicted values, while NSE assesses the model's efficiency on a scale ranging from $-\infty$ to 1, where 1 represents the most efficient model.

$$r = \frac{n(\sum xy) - (\sum x)(\sum y)}{\sqrt{\left[n\sum x^2 - (\sum x)^2\right]\left[n\sum y^2 - (\sum y)^2\right]}} \tag{6}$$

$$\text{MAE} = \frac{1}{n}\sum_{i=1}^{n}|x - y| \tag{7}$$

$$\text{NSE} = 1 - \frac{\sum(y - x)^2}{\sum(x - \bar{x})^2} \tag{8}$$

n is the number of data points, x is target value, y is predicted value.

4. Results

4.1. Coastline Analysis

Analysis of the data obtained from Sefton Council revealed rapid sediment movement and instability along most part of the Morecambe Bay coastline. Marshy areas, mudflat edges (defined as mudflat crossing zero mean sea level), and clifftops have retreated significantly, indicating rapid coastal transformation. Sediment Volume changes indicate that only a minority of sites is stable.

Figure 4 shows a selection of representative transects along Morecambe Bay for the stable, accreting, eroding and fluctuating cases. Figure 4b shows Sunderland Point in Morecambe, where according to our analysis the clifftop retreated about 5 m between 2010 and 2022. The first three profiles in Figure 4b (2010, 2012, and 2015) show significant retreat toward the landmass. As observed from Google Earth, rock armor was placed between 2013 and 2015, which reduced the retreat, as seen in its next profile in 2022. Figures 4c and 4f show the transects experiencing mudflat edge retreat. Figure 4c shows transects near Morecambe city, where mudflat edge retreated about 150 m between 2010 and 2022. Figure 4f shows transects near Bardsea, where massive erosion of about 5,012.7 m^3/m sediment has caused the mudflat edge to retreat more than 2 km between 2007 and 2022. Figure 4d, near Morecambe city, shows significant erosion of 308.06 m^3/m of sediment between 2012 and 2022. Figure 4e shows transects near Ravenstown, a mostly marshy area that has experienced significant marshland loss in recent years. The location shown in Figure 4e has seen the marshland retreat about 500 m between 2007 and 2022. Figure 4g shows transects near Baycliff that experienced short-term fluctuations in erosion between 2007 and 2022. The beach eroded between 2007 and 2017, accreted until 2021, and then eroded again in 2022. Figure 4h shows transects, near Roosebeck, between 2007 and 2022, which shows accretion of about 346.4 m^3/m of sediment resulting in the extension of mudflat edge toward the bay.

Figure 5 shows the results of a transect analysis of all locations along the Morecambe Bay coastline. The length of each line represents the length of the transect measured at each location. Locations are classified as stable, eroding, accreting, or experiencing short-term fluctuations based on sediment volume changes at each location. Volume changes are determined by subtracting the calculated sediment volume of each profile over time from the sediment volume of the initial profile measured at each location. The initial profile measurement was taken in 2010 for a few locations and in 2012 for the majority of locations.

This classification is indicated by different colored dots in Figure 5. Locations with less than 10% change in sediment volume are classified as stable. As shown in Figure 5, most marshy are classified as stable (blue). This is because transect length data is only available within marsh platform areas, where very little change is observed. Higher volume changes are noticeable for those transects extending to the mudflat and which are classified

10.1029/2024WR037523

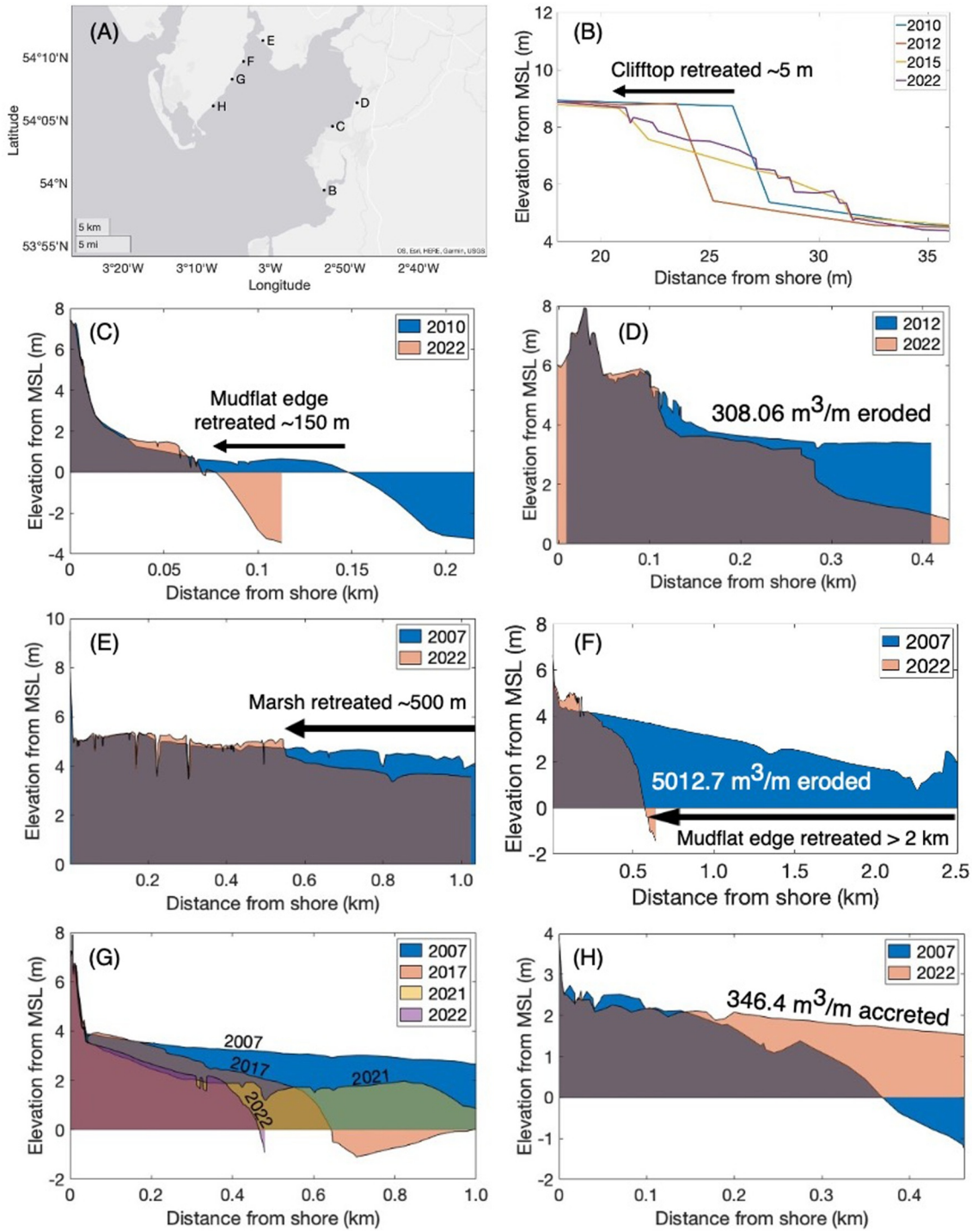

Figure 4. Beach profiles at different locations along (a) Morecambe Bay coastline; (b) near Sunderland Point; (c) near Morecambe City (mudflat); (d) near Morecambe City; (e) near Ravenstown; (f) near Bardsea; (g) near Baycliff; (h) near Roosebeck.

accordingly. For the remaining marshlands, transects extend beyond the marshland into the mudflat, recording sediment erosion from the mudflat and the retreat of the marshland. These classifications were fed to the prediction models (A1 and A2) to predict the change in volume of sediment after erosion/accretion.

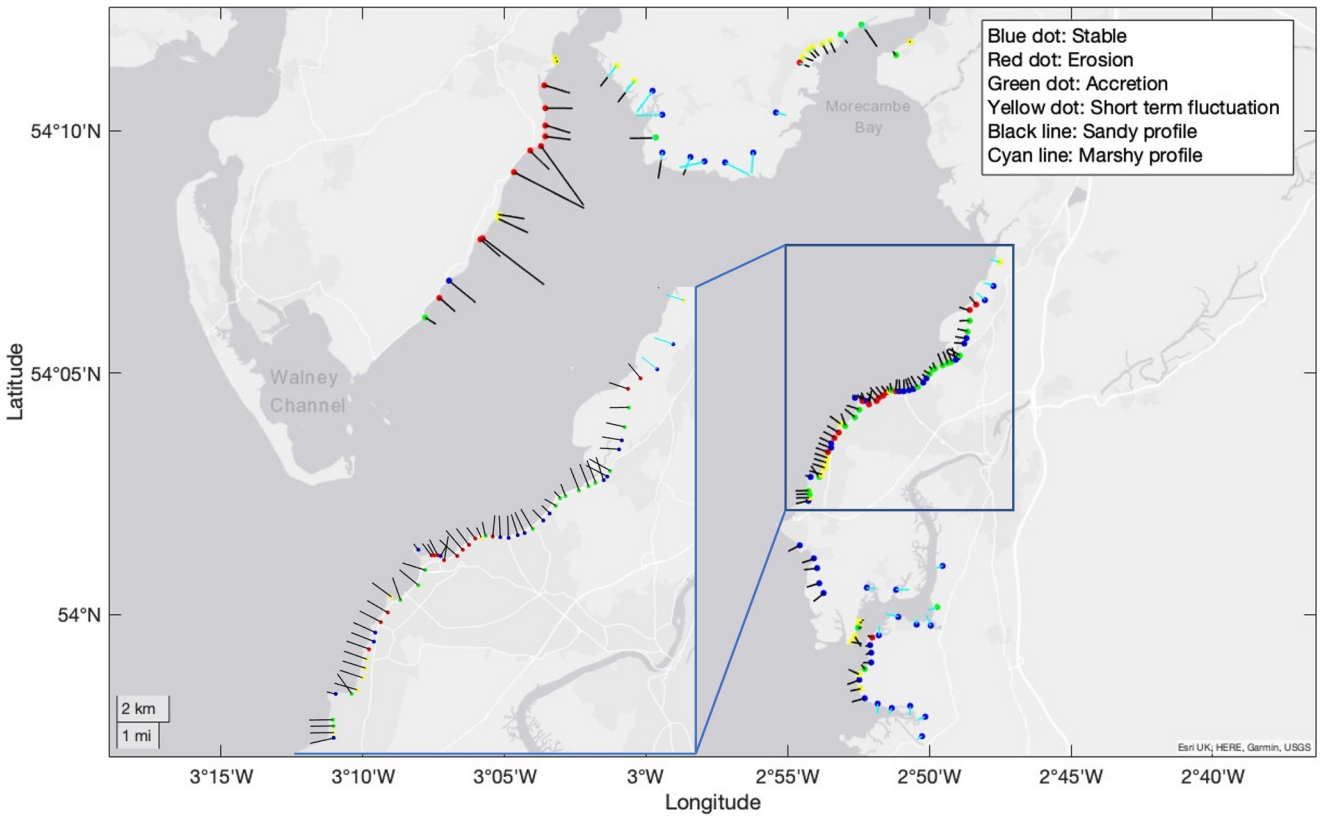

Figure 5. Beach transects at different locations along Morecambe Bay coastline illustrating sand and marsh profiles that are experiencing erosion, accretion, short-term fluctuations, and stability.

4.2. A1 Model

Model A1 was trained to classify beach behavior as eroding, accreting, stable, or undergoing short-term fluctuations based on six input parameters: coastline angle (radians), wave direction (radians), average wave height (m), maximum wave height (m), average wave velocity (m/s), and transect type (categorical, e.g., marshy). The RF classifier model was tested using various ensemble aggregation methods (bagging, AdaBoostM2, LPBoost, RUSBoost, and TotalBoost) and different numbers of trees (50, 75, and 100). 15% of the data was reserved for testing, another 15% of the data was reserved for validation and the remaining 70% was used for training. These configurations yielded good prediction performance in terms of accuracy, precision, recall, and F1 score (table 1) with 75 trees and RUSBoost method. This model effectively classifies beach behavior with training accuracy of 0.94 and testing accuracy of 0.74, providing valuable input for Model A2's prediction of sediment volume.

4.3. A2 Model

Model A2 was developed to predict the change in volume of sediment based on seven input parameters: mean and maximum wave height (m), mean wave velocity (m/s), coastline behavior (categorical output from Model A1), and the previous 18 months (three-time steps) of sediment volume (m^3/m). Three models, one LSTM and two S2S, were trained for predicting 0.5 years (one time step) ahead, 1.5 years (three time steps) and 5 years (10 time step) ahead, respectively. For the LSTM model, three and four LSTM layers were tested. The number of nodes in the LSTM layer was varied from 5 to 50. Ten percent of the data was reserved for testing, another 10% was used for validation, and the remaining 80% was used for training. All three data sets were normalized to a range between −1 and 1, and the model's performance was evaluated using the normalized data. Both models demonstrated remarkable accuracy in predicting change in sediment volume (table 2). The LSTM

Table 1
Performance of A1 Model

Criteria	Training	Testing
Accuracy	0.94	0.74
Precision	0.95	0.86
Recall	0.94	0.74
F1 Score	0.94	0.71

Table 2
Performance of A2 Model

Model	Regression			
	Training	Testing	Testing MAE (m^3/m)	Testing NSE
LSTM	0.89	0.92	0.0355	0.84
S2S (1.5 years)	0.97	0.96	0.0270	0.90
S2S (5 years)	0.99	0.88	0.0289	0.73

model achieved excellent accuracy when tested with four LSTM layers and 10 nodes in each layer, while the two S2S models achieved excellent accuracy with 20 nodes in its LSTM layers for predicting 1.5 and 5 years ahead. Model A2 predicts changes in sediment volume for future time steps relative to the sediment volume of the first time step in the time series for each location. The initial sediment volume of each location in the data set is stored alongside the model and can be added to the predicted change in sediment volume to obtain the total sediment volume at a specific location.

The S2S models predict multiple time-step values simultaneously, with Table 2 presenting the average accuracy across individual time steps. A detailed breakdown of accuracy reveals testing MAE values for t, $t + 1$, and $t + 2$ at 0.0263, 0.0260, and 0.0289, respectively, for a 1.5-year prediction. For a 5-year prediction, testing MAE values are listed as 0.0261, 0.0283, 0.0283, 0.0280, 0.0302, 0.0316, 0.0341, 0.0282, 0.0282 and 0.0259. The testing MAE is lower for longer time-step predictions compared to shorter time-step predictions, indicating that short-term fluctuations are more challenging to predict than long-term trends. This observation is reasonable, as short-term variations are frequently influenced by specific stochastic events, which differ from the broader, long-term patterns of erosion or accretion. These long-term trends, which are more pronounced over extended time series, tend to be more predictable. The S2S model is recommended for longer predictions; however, it's important to account for varying errors across time steps when using this approach.

4.4. Input Importance

LSTM and S2S models are trained using seven inputs, one of which is the output of the RF (A1) model. To assess the importance of each input in predicting the volume of sediment, we employed the Permutation Importance (PI) method. PI evaluates the significance of each input based on the variation in the model's prediction error when a specific input is shuffled (Nirmalraj et al., 2023). The PI algorithm involves selecting one input at a time and shuffling the order of its values. This shuffled input is then combined with the other inputs to create a new set of inputs, which is fed into the model to generate predictions and calculate the error. The PI of an input is determined by subtracting the baseline error (the prediction error of the model with all original inputs) from the calculated error. Figure 6 presents the normalized input importance of each input for LSTM, S2S (3 time-step) and S2S (10 time-step) model. Normalized importance is calculated by dividing each input importance by the sum of all input importance.

As shown in Figure 6, the importance of each input changes depending on the number of predicted time steps. For example, in the LSTM model, which forecasts one time step ahead, all inputs have nearly equal significance. However, in S2S models predicting 3- and 10-time steps ahead, the inputs "Volume of sediment (t-1)" and "Volume of sediment (t-3)" carry greater importance than the others. In contrast, "Volume of sediment (t-2)" appears to be less significant compared to "t-1" and "t-3" for longer-term predictions, possibly due to its limited

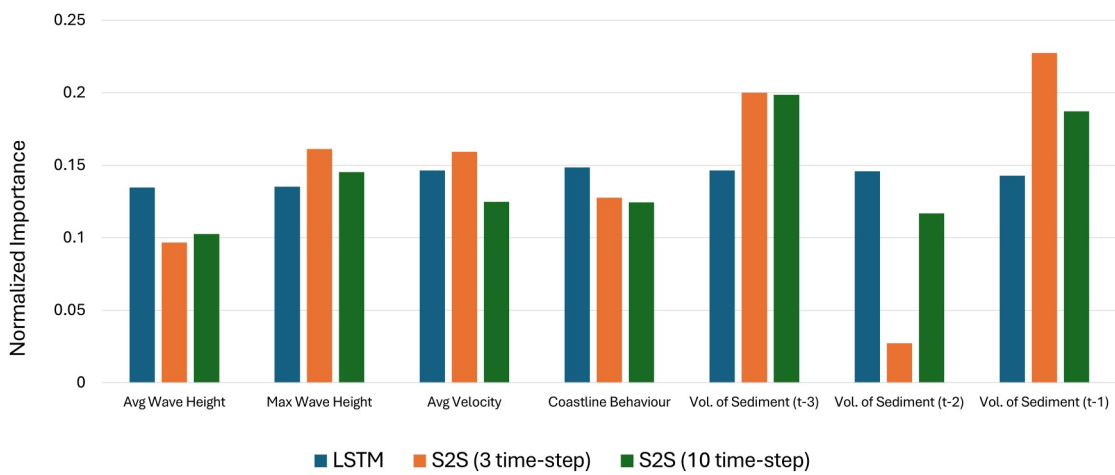

Figure 6. Input importance.

additional predictive value at these time lags. The input "Coastline behavior," which is the output of the RF (A1) model, has comparable importance in one time-step-ahead predictions, but its importance decreases as the prediction time steps increase.

5. Discussion

Coastline changes in Morecambe Bay have been observed and studied since 1990s by several researchers including Pringle (1995), Mason et al. (1999, 2010). These studies have documented significant changes in the bathymetry near the coastline. These morphological changes are primarily driven by tidal asymmetry in Morecambe Bay, where stronger currents associated with the flood tide play a key role in eroding the channels in the bay (Mason et al., 2010). The unequal duration of the semi-diurnal ebb and flood tides creates an asymmetrical tidal pattern, with the ebb lasting about 40 min longer than the flood at Heysham (COMBER et al., 1994). The bay's wave climate is dominated by smaller waves, as their size is constrained by the limited fetch due to the sheltering landmasses of Ireland, the Isle of Man, and spits at the bay's entrance (Mason et al., 2010). The flood tide reaches eroding marsh blocks and the seaward marsh cliffs, which are subjected to wave action. Although these waves are generally low-energy, generated within Morecambe Bay, south-westerly storms can bring much higher-energy waves from the Irish Sea to this coastline (Pringle, 1995). Pringle (1995) noticed the erosion of salt marshes, which began in mid-1970s and continued into the 1990s at a relatively slow rate. In addition to the erosion of salt marshes, the Kent channel of Morecambe also shifted eastward along with its minor channels during the late 1970s, leading to rapid saltmarsh erosion. Mason et al. (1999), observed the movement of the Leven estuary of Morecambe toward the north-east by about 2 km during the period of 1992–1997. Mason et al. (2010) also observed the migration of the Ulverston channel of Morecambe north-east by about 5 km between 1991 and 2004. Similarly, this study, conducted with the data between 2007 and 2022, also observed significant erosion of mudflat platforms and marshy regions in most parts of Morecambe. This erosion has resulted in the mudflat edges, that is, zero mean sea level crossing of mudflats, retreating up to 2 km (crossing of mean sea level) and marshes up to 500 m toward the landmass (Figure 4). These dynamic changes in bathymetry near the coastline pose significant challenges for the infrastructure sector and coastal communities.

The models developed in this study can effectively identify erosion hotspots and predict sediment volume changes based on simplified modeling and QGIS inputs. Model A1 is designed to classify the coastline behavior as eroding, accreting, stable or undergoing short term fluctuations based on inputs of coastline angle, wave velocity, wave direction and coastline composition. Model A2 is specifically designed to estimate the volume of sediment eroded or accreted along the coastline based on inputs of wave height, wave velocity, coastline behavior (output from Model A1), and the previous 18 months of sediment volume and at a time scale of 1.5 and 5 years.

The advantage of this methodology lies in its development of two predictive models. One of these models (model A1) is dedicated to identifying erosion hotspots, critical information for effective coastline management. This Model can be utilized to pinpoint erosive locations along the coastlines. Additionally, model A1 outputs feeds its output into the second model (model A2), enabling the latter to learn coastline classification—whether eroding, accreting, fluctuating, or stable—and subsequently predict sediment volumes in the future. Predicting sediment volumes holds regional significance as these sediments play crucial roles in beach maintenance, nearshore bank systems, and nearshore sediment transport pathways. Model A2 can thus be applied to forecast sediment erosion volumes along beaches, thereby assisting in better understanding and managing coastal erosion processes and their impacts on coastal ecosystems and communities.

Another advantage of using ANN models are that these are computationally inexpensive (Hashemi et al., 2010), as compared to the simulation models which typically require hours for simulation. Thus, the sediment volume change can be predicted instantly in the scale of 5 years. A drawback of ANN, as suggested by Hashemi et al. (2010), is that its prediction accuracy is depended on quality of data. However, this study has the advantage of training models on high quality field data.

The prediction models in this study are trained on extensive data spanning from 2010 to 2022. This period includes various storm conditions observed in Morecambe Bay. These models are capable of predicting yearly sediment volume changes. They are trained to forecast data points three and 10 steps ahead in the time series, equivalent to 1.5 and 5 years into the future respectively, using 18 months of historical sediment volume data. To further test the usability of the models, the prediction performance was evaluated across two different time scales to assess the model's ability to forecast over longer durations. Prediction results of model S2S with 10-time step is

presented in Figures 7 and 8 where this model was used to predict the change in volume of sediment ranging from 2018 Spring to 2022 Autumn based on previous three time steps (i.e., 2016 Autumn 2017 Spring and 2017 Autumn). Figure 7a shows the predicted and observed (target) volume of sediment in 2018 Spring, calculated by adding the volume of sediment of first profile in time to the predicted change in volume of sediment in 2018 Spring. Similarly, the volume of sediment for 2022 Autumn was calculated and is shown in Figure 7b. These figures represent the accurate volume of sediment predictions by S2S model. To determine the change in sediment volume between 2018 and 2022, the sediment volume in Spring 2018 was subtracted from the sediment volume in Autumn 2022, and the result was divided by the number of years, as shown in Figure 7c. The regression plots of these predicted and observed values for sediment volume in Spring 2018, sediment volume in Autumn 2022, and change in sediment volume per year from 2018 to 2022 are presented in Figures 8a and 8c, respectively. Similar figures for years 2013–2018 and 2015 to 2019 are added in Figure S2 in Supporting Information S1 (Figure S2.2 to S2.9 in Supporting Information S1).

Figure 9 presents the predicted erosion and accretion occurring over the next 5 years. These predictions were made by the S2S (10 time-step) model, using data from the last three time steps in the input, that is, 2021 Autumn 2022 Spring and 2022 Autumn. The model provided predictions for 10 time steps ahead, covering the period from 2023 to 2027. According to the predicted data, 72 out of the 125 analyzed locations are experiencing erosion, ranging from moderate to severe.

According to a report by Masselink et al. (2020), 17.3% of the UK coastline, equivalent to 3,008 km, is currently experiencing erosion. The report further notes that only 45.6% of England's coastline is protected by coastal defense structures such as groynes, seawalls, or artificial beaches. Human interventions significantly impact coastal changes, primarily by altering sediment movement in coastal areas. These interventions include coastal protection structures (such as seawalls, breakwaters, jetties, and groynes), land reclamation, construction of flood control dams, and urban development (such as building vacation homes and coastal highways). Williams et al. (2018) examined the impact of human interventions on coastal erosion along the UK coastline and in other countries, finding that harbors can lead to downdrift erosion. For example, the construction of a harbor at Port Talbot, UK, to facilitate the import of iron ore for the country's largest steelworks, caused significant erosion of the nearby Kenfig dunes. Coastal protection structures, while designed to reduce wave energy and slow coastal retreat, can lead to coastline hardening and alter sediment hydrodynamics, resulting in shifts in erosion zones toward adjacent coasts (Huang & Jin, 2018). The current study area covers Morecambe from 2007 to 2022, during which there have been no major coastal human interventions. However, significant human interventions occurred in Morecambe Bay in the past, including the construction of defenses such as stone jetties and seawalls around the jetties, and the installation of groynes between 1850 and 1900. Additionally, sea walls were built in the 1920s and 1930s, a secondary wave reflection wall was constructed in 1982, and coastal protection and flood defenses were established from 1989 to 2007 following the 1983 storm (FSC, 2020); Fish-Tail groynes were also constructed in 1992 (French & John, 2000). Human interventions within the Morecambe Bay area are limited to a small section of Morecambe city, and all of these interventions were implemented before the study period began. Consequently, there is no data available to compare conditions with and without these interventions, which is essential for training predictive models. Therefore, they were excluded from the modeling process. For future studies, these interventions can be incorporated into machine learning models by gathering relevant data on human activities and aligning historical coastline data with these interventions spatially and temporally. Key features such as type, scale, and location with respect to coastline, can be identified for each intervention. These features, along with other input parameters, can then be integrated into machine learning models to predict coastline changes influenced by human activities.

Suspended sediment concentration (SSC) plays a significant role in determining the volumetric changes in beach transects (Pang et al., 2019, 2020). The beach transect data used in this study are actual transect data, providing a realistic representation of the combined effects of SSC and sediment size. Therefore, the aspects of SSC and sediment size are not separately accounted for in this study, as the received data inherently includes their combined impact. Additionally, the simulation model developed is a hydrodynamic model rather than a morphodynamical model. This distinction means that during the simulation, the bathymetry was not allowed to update.

The prediction models developed in this study offer the advantage of providing highly accurate predictions for Morecambe Bay, as they are trained on a comprehensive field data set specific to this location. However, these models are inherently limited by their reliance on data and training derived solely from Morecambe Bay, a

10.1029/2024WR037523

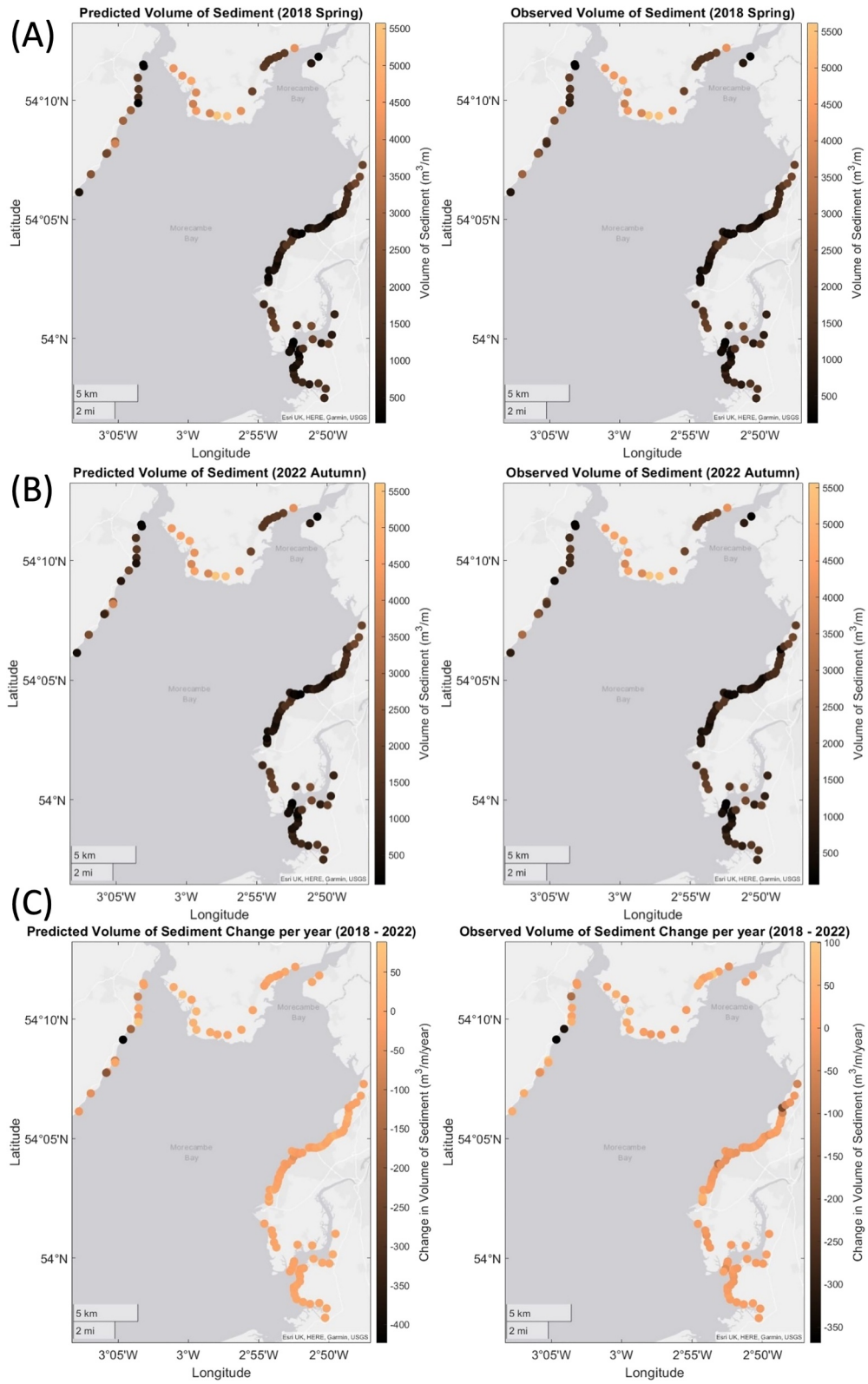

Figure 7. (a) Predicted and observed volume of sediment in 2018 Spring. (b) Predicted and observed volume of sediment in 2022 Autumn. (c) Volume of sediment change from 2018 to 2022.

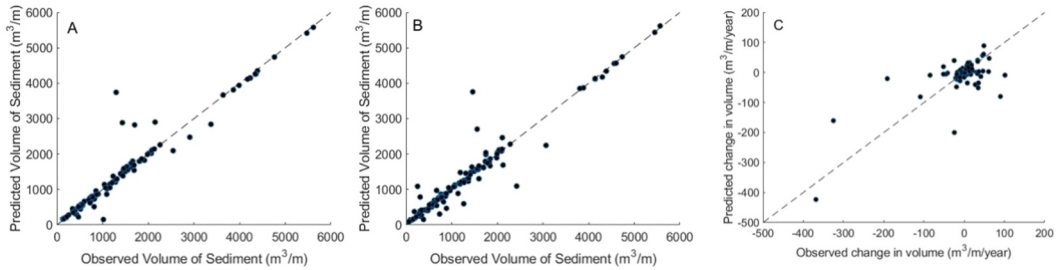

Figure 8. Regression plot for (a) volume of sediment in 2018 Spring (Regression = 0.96, MAE = 109.58 m^3/m) (b) volume of sediment in 2022 Autumn (Regression = 0.96, MAE = 128.21 m^3/m) (c) change in volume of sediment from 2018 to 2022 (Regression = 0.76, MAE = 20.98 m^3/m/year).

macrotidal embayment with a spring tidal range of 8.2 m (Mason et al., 2010). The wave climate in this region is characterized by relatively small waves, restricted by the limited fetch due to the surrounding landmasses of Ireland, the Isle of Man, and spits at the Bay's entrance. While the models exhibit exceptional predictive accuracy within this environment, further training on additional data sets would be necessary to maintain high accuracy when extending these models and their structure to other regions. To the authors' knowledge, this is the first study to propose a two-stage modeling framework based on Long Short-Term Memory (LSTM) and Sequence-to-Sequence (S2S) models for predicting morphological changes along a coastline.

Future developments of these models will involve incorporating additional historical data, enabling the models to scale up and provide forecasts for even longer time horizons. Moreover, enhancing the input list with additional features should enhance prediction capabilities by enabling models to grasp the relationship between coastal erosion and various variables. As demonstrated by Peponi et al. (2019), factors such as urbanization and population influence coastal dynamics systems by modifying hydrological patterns, sedimentation regimes, land use and land cover. Additionally, coastal erosion is influenced by rising sea levels and sediment size (Masselink et al., 2020). Thus, incorporating these factors into the model's input list will facilitate learning the relationship between sediment erosion along the coastline and these variables, ultimately enhancing the model's predictive robustness.

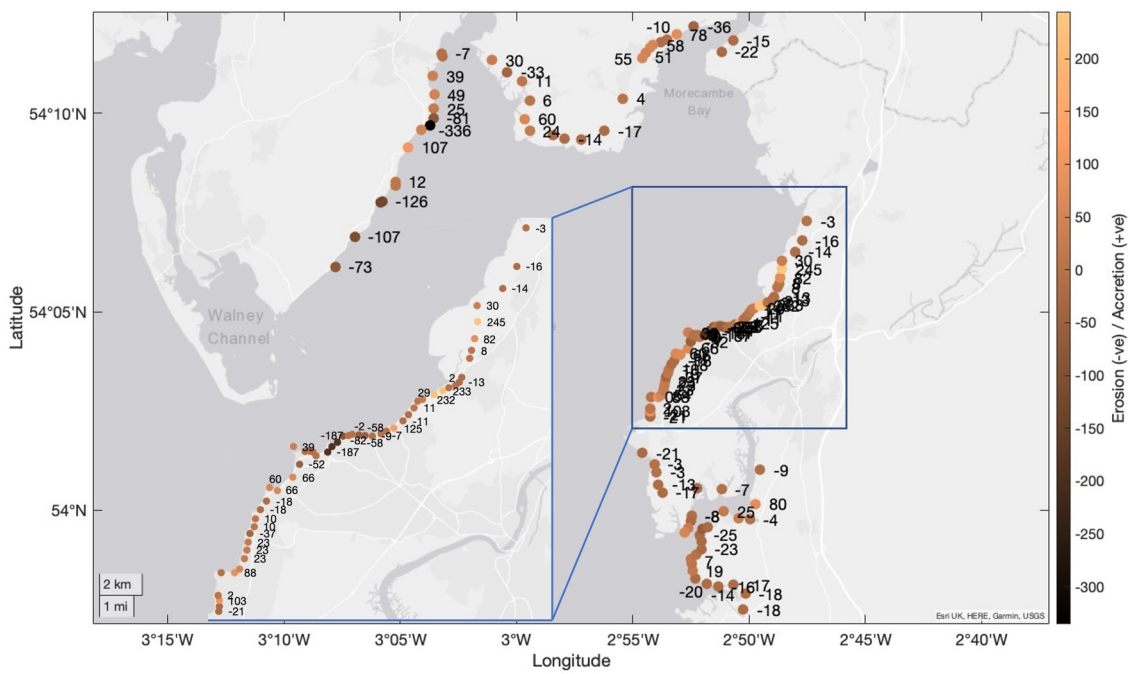

Figure 9. Erosion/Accretion (m^3/m) of along Morecambe Bay in next five years (2023–2027).

6. Conclusion

This study analyzes field data comprising beach transects at 125 locations along the Morecambe Bay coastline. The analysis reveals areas of rapid coastal change. Following the data analysis, this study investigates the potential of a two-stage machine learning model for predicting sediment volume change in a coastal environment. The model utilized a combination of beach behavior classification and deep learning techniques to achieve accurate predictions. The results demonstrated that the model effectively captured the complex relationship between beach behavior, wave conditions, and sediment erosion and accretion.

Model A1 successfully classified beach behavior into four categories: eroding, accreting, stable, and undergoing short-term fluctuations using Random Forests and based on input of coastline angle, wave velocity, wave direction and coastline composition. This classification provided valuable input for Model A2, which utilized LSTM and sequence-to-sequence models to predict change in sediment volume for one-step-ahead and multi-step-ahead predictions, respectively. The Permutation Importance (PI) method shows that for predicting coastline behaviors 6 months into the future, the inputs of average wave height, maximum wave height, wave velocity, sediment volume under the curve, and coastline classification (e.g., eroding vs. accreting) hold similar levels of importance in the data-driven models. However, when forecasting 0.5 and 5 years ahead, volume of sediment at time step t-1 and t-3 becomes the most critical input. The random forest classifier achieves testing accuracy of 0.74. The LSTM model achieved a testing regression score of 0.92 for one-step-ahead (6 months) predictions of the available sediment volume time series. Similarly, the sequence-to-sequence models achieved a testing regression score of 0.96 and 0.88 for both three-time-step-ahead (1.5 years) predictions and ten-time-step-ahead (5 years) predictions, respectively. Proposed models offer several advantages over traditional time series models. Firstly, it explicitly classifies beach behavior based on input of coastline angle, wave velocity, wave direction, and coastline composition. Secondly, the model is highly generalizable and can be applied to different coastal environments with minimal adjustments.

Data Availability Statement

The data obtained from the Sefton Council for this study is available through Kumar and Leonardi (2024b).

Acknowledgments
We acknowledge the following funding source for this study: Engineering with Nature: combining Artificial intelligence, Remote sensing and computer Models for the optimum design of coastal protection schemes EP/V056042/1. We acknowledge Paul Wisse, Samantha Godfrey-Lord, Andrew Martin and Michelle Barnes from Sefton Council for providing data from the coastal monitoring program.

References

Adamo, F., De Capua, C., Filianoti, P., Lanzolla, A. M. L., & Morello, R. (2014). A coastal erosion model to predict shoreline changes. *Measurement*, *47*, 734–740. https://doi.org/10.1016/j.measurement.2013.09.048

Anctil, F., Filion, M., & Tournebize, J. (2009). A neural network experiment on the simulation of daily nitrate-nitrogen and suspended sediment fluxes from a small agricultural catchment. *Ecological Modelling*, *220*(6), 879–887. https://doi.org/10.1016/j.ecolmodel.2008.12.021

Aslam, M., Lee, J.-M., Kim, H.-S., Lee, S.-J., & Hong, S. (2020). Deep learning models for long-term solar radiation forecasting considering microgrid installation: A comparative study. *Energies*, *13*(1), 147. https://doi.org/10.3390/en13010147

Betzold, C., & Mohamed, I. (2017). Seawalls as a response to coastal erosion and flooding: A case study from grande comore, Comoros (West Indian Ocean). *Regional Environmental Change*, *17*(4), 1077–1087. https://doi.org/10.1007/s10113-016-1044-x

Boettle, M., Rybski, D., & Kropp, J. P. (2013). How changing sea level extremes and protection measures alter coastal flood damages. *Water Resources Research*, *49*(3), 1199–1210. https://doi.org/10.1002/wrcr.20108

Breiman, L. (2001). Random forests. *Machine Learning*, *45*(1), 5–32. https://doi.org/10.1023/a:1010933404324

Browder, A. E., Dean, R. G., & Chen, R. (2015). Performance of a submerged breakwater for shore protection. *Coastal Engineering*, *25*(1996), 2312–2323. https://doi.org/10.1061/9780784402429.179

Comber, D. P. M., Hansom, J. D., Nature, E., & Group, G. U. C. R. (1994). Estuaries management plans, coastal processes and conservation: Morecambe Bay: Recommendations.

Corbella, S., & Stretch, D. D. (2012). Predicting coastal erosion trends using non-stationary statistics and process-based models. *Coastal Engineering*, *70*, 40–49. https://doi.org/10.1016/j.coastaleng.2012.06.004

Crawford, T. W., Islam, M. S., Rahman, M. K., Paul, B. K., Curtis, S., Miah, M. G., & Islam, M. R. (2020). Coastal erosion and human perceptions of revetment protection in the lower meghna estuary of Bangladesh. *Remote Sensing*, *12*(18), 3108. https://doi.org/10.3390/rs12183108

Dionísio António, S., van der Werf, J., Horstman, E., Cáceres, I., Alsina, J., van der Zanden, J., & Hulscher, S. (2023). Influence of beach slope on morphological changes and sediment transport under irregular waves. *Journal of Marine Science and Engineering*, *11*(12), 2244. https://doi.org/10.3390/jmse11122244

Farzad, F., & El-Shafie, A. H. (2017). Performance enhancement of rainfall pattern – Water level prediction model utilizing self-organizing-map clustering method. *Water Resources Management*, *31*(3), 945–959. https://doi.org/10.1007/s11269-016-1556-7

Forrester, J., Leonardi, N., Cooper, J. R., & Kumar, P. (2024). Seagrass as a nature-based solution for coastal protection. *Ecological Engineering*, *206*, 107316. https://doi.org/10.1016/j.ecoleng.2024.107316

French, P. W., & John, S. L. (2000). The impacts of fish-tail groynes on sediment deposition at Morecambe, North-West England. *Journal of Coastal Research*, *16*(3), 724–734. Retrieved from http://www.jstor.org/stable/4300082

Fsc, C. H. (2020). Morecambe: A History of Storm Damage and Coastal Defence. Retrieved from https://arcg.is/10Tfz0

Harris, L. E. (2012). Submerged reef structures for beach erosion control. In *Coastal Structures 2003* (pp. 1155–1163).

Hashemi, M. R., Ghadampour, Z., & Neill, S. P. (2010). Using an artificial neural network to model seasonal changes in beach profiles. *Ocean Engineering*, *37*(14), 1345–1356. https://doi.org/10.1016/j.oceaneng.2010.07.004

Huang, Y., & Jin, P. (2018). Impact of human interventions on coastal and marine geological hazards: A review. *Bulletin of Engineering Geology and the Environment*, *77*(3), 1081–1090. https://doi.org/10.1007/s10064-017-1089-1

Kim, J., Yun, J.-H., & Kim, H. C. (2020). Anomaly detection for industrial control systems using sequence-to-sequence neural networks. In *Paper presented at the Computer Security, Cham*.

Kumar, P., Ahmed, A. N., Sherif, M., Sefelnasr, A., & Elshafie, A. (2023). Development of long short-term memory model for prediction of water table depth in United Arab Emirates. In M. Sherif, V. P. Singh, A. Sefelnasr, & M. Abrar (Eds.), *Water Resources Management and Sustainability: Solutions for Arid Regions* (pp. 141–152). Springer Nature Switzerland.

Kumar, P., & Leonardi, N. (2023a). Coastal forecast through coupling of Artificial Intelligence and hydro-morphodynamical modelling. *Coastal Engineering Journal*, *65*(3), 1–20. https://doi.org/10.1080/21664250.2023.2233724

Kumar, P., & Leonardi, N. (2023b). Exploring mega-nourishment interventions using long short-term memory (LSTM) models and the sand engine surface MATLAB framework. *Authorea*. https://doi.org/10.22541/au.169297181.19761587/v1

Kumar, P., & Leonardi, N. (2023c). A novel framework for the evaluation of coastal protection schemes through integration of numerical modelling and artificial intelligence into the Sand Engine App. *Scientific Reports*, *13*(1), 8610. https://doi.org/10.1038/s41598-023-35801-5

Kumar, P., & Leonardi, N. (2024a). Exploring mega-nourishment interventions using long short-term memory (LSTM) models and the sand engine surface MATLAB framework. *Geophysical Research Letters*, *51*(4), e2023GL106042. https://doi.org/10.1029/2023GL106042

Kumar, P., & Leonardi, N. (2024b). High-Resolution Beach Profile Time Series: Morecambe Bay, 2007–2022 [Dataset]. https://doi.org/10.5281/zenodo.10907660

Lima, M., Coelho, C., Veloso-Gomes, F., & Roebeling, P. (2020). An integrated physical and cost-benefit approach to assess groins as a coastal erosion mitigation strategy. *Coastal Engineering*, *156*, 103614. https://doi.org/10.1016/j.coastaleng.2019.103614

Lindemann, B., Maschler, B., Sahlab, N., & Weyrich, M. (2021). A survey on anomaly detection for technical systems using LSTM networks. *Computers in Industry*, *131*, 103498. https://doi.org/10.1016/j.compind.2021.103498

Lyddon, C. E., Brown, J. M., Leonardi, N., Saulter, A., & Plater, A. J. (2019). Quantification of the uncertainty in coastal storm hazard predictions due to wave-current interaction and wind forcing. *Geophysical Research Letters*, *46*(24), 14576–14585. https://doi.org/10.1029/2019GL086123

Mason, D. C., Amin, M., Davenport, I. J., Flather, R. A., Robinson, G. J., & Smith, J. A. (1999). Measurement of recent intertidal sediment transport in Morecambe Bay using the waterline method. *Estuarine, Coastal and Shelf Science*, *49*(3), 427–456. https://doi.org/10.1006/ecss.1999.0508

Mason, D. C., Scott, T. R., & Dance, S. L. (2010). Remote sensing of intertidal morphological change in Morecambe Bay, U.K., between 1991 and 2007. *Estuarine, Coastal and Shelf Science*, *87*(3), 487–496. https://doi.org/10.1016/j.ecss.2010.01.015

Masselink, G., Russell, P., Rennie, A., Brooks, S., & Spencer, T. (2020). Impacts of climate change on coastal geomorphology and coastal erosion relevant to the coastal and marine environment around the UK. *MCCIP Science Review*, *2020*, 158–189.

MetOffice. (2014). 12 February 2014—Storm statistics. Retrieved from https://wp.me/pYUo9-1PC

MetOffice. (2016). UK storm season 2015/16. Retrieved from https://www.metoffice.gov.uk/weather/warnings-and-advice/uk-storm-centre/uk-storm-season-2015-16

MetOffice. (2020). Storm Ciara. Retrieved from https://www.metoffice.gov.uk/weather/warnings-and-advice/uk-storm-centre/storm-ciara

Muñoz, D. F., Moftakhari, H., & Moradkhani, H. (2020). Compound effects of flood drivers and wetland elevation correction on coastal flood hazard assessment. *Water Resources Research*, *56*(7), e2020WR027544. https://doi.org/10.1029/2020WR027544

Nirmalraj, S., Antony, A. S. M., Srideviponmalar, P., Oliver, A. S., Velmurugan, K. J., Elanangai, V., & Nagarajan, G. (2023). Permutation feature importance-based fusion techniques for diabetes prediction. *Soft Computing*. https://doi.org/10.1007/s00500-023-08041-y

Pang, W., Dai, Z., Ge, Z., Li, S., Mei, X., Gu, J., & Huang, H. (2019). Near-bed cross-shore suspended sediment transport over a meso-macro tidal beach under varied wave conditions. *Estuarine, Coastal and Shelf Science*, *217*, 69–80. https://doi.org/10.1016/j.ecss.2018.11.007

Pang, W., Dai, Z., Ma, B., Wang, J., Huang, H., & Li, S. (2020). Linkage between turbulent kinetic energy, waves and suspended sediment concentrations in the nearshore zone. *Marine Geology*, *425*, 106190. https://doi.org/10.1016/j.margeo.2020.106190

Pang, W., Ge, Z., Dai, Z., Li, S., & Huang, H. (2021). The behaviour of beach elevation contours in response to different wave energy environments. *Earth Surface Processes and Landforms*, *46*(2), 443–454. https://doi.org/10.1002/esp.5036

Peponi, A., Morgado, P., & Trindade, J. (2019). Combining artificial neural networks and GIS fundamentals for coastal erosion prediction modeling. *Sustainability*, *11*(4), 975. https://doi.org/10.3390/su11040975

Pham, Q. B., Kumar, M., Di Nunno, F., Elbeltagi, A., Granata, F., Islam, A. R. M. T., et al. (2022). Groundwater level prediction using machine learning algorithms in a drought-prone area. *Neural Computing & Applications*, *34*(13), 10751–10773. https://doi.org/10.1007/s00521-022-07009-7

Pinto, C. A., Taborda, R., Andrade, C., Baptista, P., Silva, P. A., Mendes, D., & Pais-Barbosa, J. (2022). Morphological development and behaviour of a shoreface nourishment in the Portuguese western coast. *Journal of Marine Science and Engineering*, *10*(2), 146. https://doi.org/10.3390/jmse10020146

Prasad, D. H., & Kumar, N. D. (2014). Coastal erosion Studies°™A review. *International Journal of Geosciences*, *05*(03), 5–345. https://doi.org/10.4236/ijg.2014.53033

Pringle, A. W. (1995). Erosion of a cyclic saltmarsh in Morecambe Bay, North-West England. *Earth Surface Processes and Landforms*, *20*(5), 387–405. https://doi.org/10.1002/esp.3290200502

Ray, R. D. (1999). *A Global Ocean Tide Model From TOPEX/POSEIDON Altimetry: GOT99.2* (Vol. 58). NASA Technical Memorandum.

Rodriguez-Galiano, V., Sanchez-Castillo, M., Chica-Olmo, M., & Chica-Rivas, M. (2015). Machine learning predictive models for mineral prospectivity: An evaluation of neural networks, random forest, regression trees and support vector machines. *Ore Geology Reviews*, *71*, 804–818. https://doi.org/10.1016/j.oregeorev.2015.01.001

Sharma, V., Negi, S. C., Rudra, R. P., & Yang, S. (2003). Neural networks for predicting nitrate-nitrogen in drainage water. *Agricultural Water Management*, *63*(3), 169–183. https://doi.org/10.1016/s0378-3774(03)00159-8

Stammer, D., Ray, R. D., Andersen, O. B., Arbic, B. K., Bosch, W., Carrère, L., et al. (2014). Accuracy assessment of global barotropic ocean tide models. *Reviews of Geophysics*, *52*(3), 243–282. https://doi.org/10.1002/2014RG000450

Sun, J., Hu, L., Li, D., Sun, K., & Yang, Z. (2022). Data-driven models for accurate groundwater level prediction and their practical significance in groundwater management. *Journal of Hydrology*, *608*, 127630. https://doi.org/10.1016/j.jhydrol.2022.127630

Tang, Y., Xu, J., Matsumoto, K., & Ono, C. (2016). Sequence-to-Sequence model with attention for time series classification. In *Paper presented at the 2016 IEEE 16th International Conference on Data Mining Workshops (ICDMW)*.

van Rijn, L. C. (2011). Coastal erosion and control. *Ocean and Coastal Management*, *54*(12), 867–887. https://doi.org/10.1016/j.ocecoaman.2011.05.004

Wei, A., Chen, Y., Li, D., Zhang, X., Wu, T., & Li, H. (2022). Prediction of groundwater level using the hybrid model combining wavelet transform and machine learning algorithms. *Earth Science Informatics*, *15*(3), 1951–1962. https://doi.org/10.1007/s12145-022-00853-0

Williams, A. T., Rangel-Buitrago, N., Pranzini, E., & Anfuso, G. (2018). The management of coastal erosion. *Ocean and Coastal Management*, *156*, 4–20. https://doi.org/10.1016/j.ocecoaman.2017.03.022

Xiong, Y., Dai, Z., Long, C., Liang, X., Lou, Y., Mei, X., et al. (2024). Machine learning-based examination of recent mangrove forest changes in the western irrawaddy river Delta, Southeast Asia. *Catena*, *234*, 107601. https://doi.org/10.1016/j.catena.2023.107601

Yang, J., Dai, Z., Lou, Y., Mei, X., & Fagherazzi, S. (2023). Image-based machine learning for monitoring the dynamics of deltaic islands in the Atchafalaya River Delta Complex between 1991 and 2019. *Journal of Hydrology*, *623*, 129814. https://doi.org/10.1016/j.jhydrol.2023.129814

Yin, J., Lin, N., & Yu, D. (2016). Coupled modeling of storm surge and coastal inundation: A case study in New York city during hurricane sandy. *Water Resources Research*, *52*(11), 8685–8699. https://doi.org/10.1002/2016WR019102